Vol 14 No 4, April 2005
1009-1963/2005/14(04)/0796-06

Chinese Physics

© 2005 Chin. Phys. Soc.
and IOP Publishing Ltd

Near-field x-ray phase contrast imaging and phase retrieval algorithm*

Zhu Hua-Feng(朱化凤)†, Xie Hong-Lan(谢红兰), Gao Hong-Yi(高鸿奕), Chen Jian-Wen(陈建文), Li Ru-Xin(李儒新), and Xu Zhi-Zhan(徐至展)

Shanghai Institute of Optics and Fine Mechanics, Chinese Academy of Sciences, Shanghai 201800, *China*

(Received 2 July 2004; revised manuscript received 29 November 2004)

Theoretical analyses of x-ray diffraction phase contrast imaging and near field phase retrieval method are presented. A new variant of the near field intensity distribution is derived with the optimal phase imaging distance and spatial frequency of object taken into account. Numerical examples of phase retrieval using simulated data are also given. On the above basis, the influence of detecting distance and polychroism of radiation on the phase contrast image and the retrieved phase distribution are discussed. The present results should be useful in the practical application of in-line phase contrast imaging.

Keywords: x-ray, phase contrast imaging, phase retrieval, diffraction
PACC: 6180C, 4230K, 4230N

1. Introduction

For 100 years x-ray imaging has depended almost wholly on the phenomenon of absorption by an object to produce contrast, which is only effective in absorbing samples. The contrast results from the varying index of absorption in the object owing to the differences in composition, thickness and density. The heavier the element, the easier it is to produce the contrast. However, with the development of medical and material sciences and bioscience, imaging based on absorption contrast can no longer be effective, because an object composed of light elements absorbs little or no x-rays, or the absorption difference between different light elements of the object is small, which leads to an indiscernible absorption contrast image. The absorption contrast can be enhanced by prolonging the exposure time, but this always results in radiation damage to the object, especially biological tissues. A new imaging technique should be developed to satisfy the requirements in the imaging of light-element-based objects. The interaction cross section of the x-ray phase shift is about one thousand times larger than that of absorption in the hard x-ray range, which implies that the phase contrast imaging has much higher sensitivity for light elements than the absorption-contrast x-ray imaging, so that the dose of absorption by the sample can be reduced and the radiation damage can be greatly decreased. This feature is very attractive from a biological point of view, because structures inside biological soft tissues consisting of light elements can be resolved without using any reference medium.

X-ray phase contrast imaging developed rapidly in the 1990s with the increasing use of synchrotron sources. So far, various methods for x-ray phase-contrast imaging have been proposed and demonstrated, including monolithic x-ray interferometers,[1−3] double-crystal diffraction arrangements,[4−7] and Fresnel diffraction from a monochromatic wave.[8−12] They are, respectively, based on the measuring of φ, $\nabla\varphi$ and $\nabla^2\varphi$, where φ is the phase shift introduced by the object. The interferometer method can give information about the phase directly. Diffraction-enhanced arrangements are suitable for the measuring of an object with slow phase variation. The Fresnel diffraction one is similar to Fresnel in-line holography and measures the edge-enhanced phase contrast image. The latter one proposed by Wilkins and co-workers[13,14] and Snigirev and co-workers[15] is preferable in research and medi-

*Project supported by the National Natural Science Foundation of China (Grant No 60278030).
†E-mail: huafengzhu@mail.siom.ac.cn

cal fields because of its simple geometry and relatively simpler technical requirements in operation. Theoretically, the maximal phase contrast occurs at $Z_R = 1/(2\lambda\mu^2)$, (where Z_R is the detecting distance at which the optimal phase contrast can be produced[14], μ is the spatial frequency characterizing the object (feature spatial frequency) of sample and λ is the x-ray wavelength), but the contrast consideration alone is insufficient to obtain optimal visibility of the phase contrast image. If the detecting distance is too small, though the resolution turns out to be good enough, the interference between the directly propagated part of x-ray and the refracted part cannot bring adequate contrast into the image; if the detecting distance is large enough to give maximum contrast, the resolution becomes too low to obtain a good visible image. Thus both resolution and contrast should be compromised in order to obtain the best visibility of phase contrast image. Another problem is that the directly measured image is only the edge-enhanced one and cannot give the whole phase distribution, which is also of great concern in many fields. Many phase retrieval algorithms are proposed and demonstrated.[16−19] Many research results reported involve qualitative discussion about the effects of the detecting distance and polychromatic radiation on the visibility of the phase contrast image, but no quantitative results are given, and there are no reports about the influences of polychromatic radiation on the retrieved phase, either. In this paper, we give quantitative results to the former and qualitative description to the latter.

In Section 2, the near-field phase contrast imaging theory is developed in a new form. Section 3 shows the phase retrieval process based on the solution of TIE (Transport of Intensity Equation) involving wavelength difference. In Section 4, computer simulation results of simulated objects are given which can be used to visualize our theory proposed in Sections 2 and 3.

2. Theory of phase contrast imaging

Let a thin object lying in the plane z=0 be illuminated with a plane wave $U_0(r_\perp, z)$ propagating along the optic axis z. The transmission function of an object $p(r_\perp,0)$ is assumed to be in the form

$$p(r_\perp, 0) = \exp\left[\mathrm{i}\varphi(r_\perp, 0) - \mu(r_\perp, 0)\right]. \tag{1}$$

In the Fresnel approximation, the complex amplitude in the observing plane can be written as

$$\begin{aligned} U_Z(r_\perp, z) =& \frac{\exp(\mathrm{i}kz)}{\mathrm{i}\lambda z} \\ &\times \exp\left[\mathrm{i}\frac{k}{2z}(r'^2_\perp, z)\right] \iint_\sigma U_1(r_\perp, 0) \\ &\times \exp\left[\mathrm{i}\frac{k}{2z}(r^2_\perp)\right] \\ &\times \exp\left[\mathrm{i}\frac{2\pi}{\lambda z}(r_\perp \cdot r'_\perp)\right] \mathrm{d}x\mathrm{d}y, \end{aligned} \tag{2}$$

where $r_\perp$=(x, y), $k = 2\pi/\lambda$ is the wave number, $U_1(r_\perp, 0) = p(r_\perp,0)U_0(r_\perp, z)$. If the Fresnel number is large enough, the high-order terms can be omitted, and then we obtain the simplified intensity distribution in the image plane[20]

$$I_Z(r_\perp, z) \approx \left|\left(1 + \frac{\mathrm{i}\lambda z}{4\pi}\nabla^2_\perp\right) U_1(r_\perp, 0)\right|^2. \tag{3}$$

Let us now consider a weak phase object, ($\mu(r_\perp$,0) =0), Eq.(3) can be rewritten as

$$\begin{aligned} I_Z(r_\perp, z) =& 1 + \frac{\lambda z}{2\pi}\nabla^2_\perp \varphi(r_\perp, z), \\ =& 1 + \frac{1}{4\pi\mu^2}\left(\frac{z}{\alpha}\right)\nabla^2_\perp \varphi(r_\perp, z), \end{aligned} \tag{4}$$

where $\nabla^2_\perp = \partial^2_x + \partial^2_y$ is the two-dimensional Laplacian, μ is the spatial frequency of a sample, and $\alpha = Z_R/10$, $Z_R = 1/(2\lambda\mu^2)$. Equation (4) indicates that the contrast of image is proportional to the Laplacian of the phase distribution. The features of the projected phase are shown in the form of enhanced edge contrast.

In the following discussion, we assume the sample to be a pure phase object.

3. Phase retrieval method based on transport of intensity equation

In the Fresnel approximation with the optical axis parallel to the z axis, the slowly varying component of the scalar monochromatic wave $U_0(r_\perp, z)$ satisfies the paraxial equation

$$(2\mathrm{i}k\partial_z + \nabla^2_\perp)U_1(r_\perp, z) = 0, \tag{5}$$

where $\partial_z = \partial/\partial z$. Considering the imaginary part of Eq.(5), we obtain[21]

$$k\partial_z I(r_\perp, z) = -\nabla \cdot \left[I\nabla\varphi(r_\perp, z)\right], \tag{6}$$

where ∇ is the gradient operator in the plane. Equation (6) is what we called TIE, proposed first by Teague.

The distribution of phase φ in the plane orthogonal to the optic axis and located immediately after a thin weakly refracting object can be expressed as follows in terms of line integral of the complex index of refraction $n \equiv 1-\delta-\mathrm{i}\beta$, $|n-1| \ll 1$, where δ is the phase shift term and β is the absorption term:

$$\varphi(r_\perp, 0, \lambda) = -(2\pi/\lambda)\int_{-\infty}^{0} \delta\left(r_\perp, z', \lambda\right)\mathrm{d}z'. \qquad (7)$$

The dependence of the real parts of the complex index on the wavelength of the incident radiation in the absence of absorption edges, for any elements present in the sample, is well known to be[22]

$$\delta(\lambda) = \left(\lambda/\lambda_0\right)^2 \delta\left(\lambda_0\right). \qquad (8)$$

Taking Eqs.(7) and (8) into account, Eq.(6) can be rewritten as

$$-\nabla^2\varphi\left(r_\perp, 0, \lambda_0\right) = \frac{k_0}{\sigma^2}\left[I\left(r_\perp, z, \lambda\right)/I\left(r_\perp, 0, \lambda\right) - 1\right], \qquad (9)$$

where σ=λ/λ_0 and k=$2\pi/\lambda_0$.

In a rectangular region $\Xi(0,a)\times(0,b)$, we introduce the Fourier harmonics H_{mn} and the standard scalar product:[23]

$$H_{mn}(x,y) = \exp\left(\frac{\mathrm{i}2\pi m x}{a}\right)\exp\left(\frac{\mathrm{i}2\pi n x}{b}\right), \qquad (10)$$

$$\langle A, H\rangle = \frac{1}{ab}\int_0^a\int_0^b A\left(x,y\right)H^*\left(x,y\right)\mathrm{d}x\mathrm{d}y, \qquad (11)$$

where m, n satisfy $|m| \le M$ and $|n| \le N$ respectively, and the star * represents the complex conjugate. M and N are large enough for the retrieval of phase. $H_{mn}(x,y)$ builds up a complete orthonormal set in Ξ. Then Eq.(7) is simplified as[23]

$$\begin{aligned}&\sum_{i,j}\varphi_{i,j}\left(r_\perp, 0, \lambda_0\right)M_{m,n}^{i,j}\\ =&abF_{m,n}, (|m| \le M, |n| \le N, m^2+n^2 > 0,\\ &i^2+j^2 > 0),\end{aligned} \qquad (12)$$

where

$$\varphi_{i,j} = \langle\varphi, H_{i,j}\rangle_{ab}, \quad F_{m,n} = \langle F, H_{m,n}\rangle_{ab}$$

which are the Fourier coefficients of φ and F respectively $\left(F = \frac{k_0}{\sigma^2}\left[\frac{I\left(r_\perp, z, \lambda\right)}{I\left(r_\perp, 0, \lambda\right)} - 1\right]\right)$, $M_{m,n}^{i,j} = (2\pi)^2\left(\mathrm{i}mb/a + jna/b\right)I_{m-i,n-j}$, and $I_{p,q} = \langle I, H_{p,q}\rangle$ which is the Fourier coefficient of intensity distribution $I(r_\perp, z,\lambda)$. The Fourier coefficient φ can be expressed as[23]

$$\varphi_{i,j}\left(r_\perp, 0, \lambda_0\right) = ab\sum_{m,n}\left[M_{m,n}^{i,j}\right]^{-1}F_{m,n}. \qquad (13)$$

In the specific case of a uniform intensity distribution where $I(x,\ y,\ 0)\equiv I_0$ in Ξ_{ab} and $I(x,y,0) \equiv 0$ both outside Ξ_{ab} and at the boundary, and $a = b$, Eq.(13) is reduced to the simplified form[23]

$$\varphi_{i,j}\left(r_\perp, 0, \lambda_0\right) = \frac{a^2}{\left(2\pi a\right)^2\left(m^2+n^2\right)I_0}. \qquad (14)$$

Then the phase can be finally obtained by

$$\varphi\left(r_\perp, 0, \lambda_0\right) = \sum_{m,n}\varphi_{m,n}H_{m,n}. \qquad (15)$$

4. Simulation experiments of phase contrast image and retrieved phase

We now present numerical examples with simulated data to help illustrate the theoretical results obtained in the previous sections.

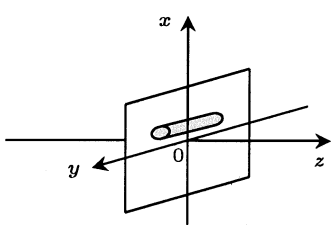


Fig.1. A fibre in the detection plane.

First, let the incident wave be a uniform monochromatic plane wave with a wavelength of λ_0=0.1nm. A fibre with a diameter of $2R$=640μm is parallel to the y axis as shown in Fig.1. The axis of the fibre is $2R$ away from the coordinate origin. The absorption of x-ray by the fibre can be neglected in a range Ξ being (0,4R) $\times$ (0,4R). The required feature is assumed to have a feature spatial frequency of (1/10) $\mu\mathrm{m}^{-1}$, then α in Eq.(4) has a value of α=Z_R/10 =$1/(20\lambda\mu^2)$=5cm.

We calculated the intensity distribution $I_z(r_\perp, z)$ in the image plane by computing the Fresnel integral (2) and used the computed intensity distribution and the method given in Section 3 to reconstruct a phase on a grid with 128 $\times$ 128 pixels. The obtained intensity distribution $I_z(r_\perp, z)$ and the retrieved phase distribution with the ratio of detecting distance z to α being 1, 0.8, 3, 5 respectively are presented in Fig.2. Obviously, when z=α, the intensity distribution has

the sharpest feature (corresponding to the best visibility) and the retrieved phase is very close to the original one. A lager or smaller detecting distance can introduce a larger aberration to the retrieved phase. Then we define $\alpha=1/\ (20\lambda\mu^2)$ as the optimal phase imaging distance which is clearly related to the incident wavelength λ and feature spatial frequency μ.

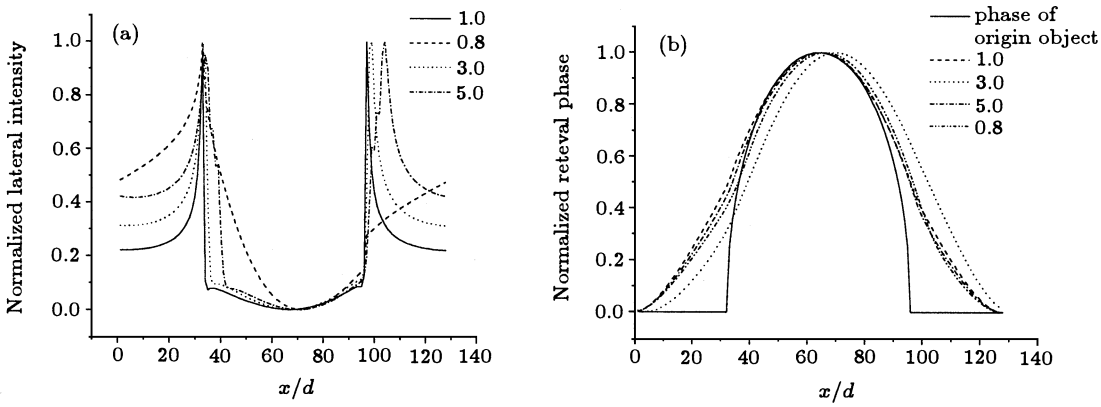


Fig.2. Intensity distribution of phase contrast image (a) and retrieved phase distribution (b) with z/α=1, 0.8, 3, 5 respectively. The incident wave is a perfectly monochromatic uniform plane wave with a wavelength of 0.1nm. For a comparison, the solid curve in (b) is the original phase distribution of the fibre. z is the distance between the detector and the sample, and α is the optimal phase imaging distance.

At the next stage, we analyse the retrieval of phase from the image intensity containing various levels of multi-energy. Now we perform the retrieval of the phase corresponding to a wavelength of λ_0(=0.1nm) which is called central wavelength. The wavelength used in the experiment is λ, then the relative wavelength difference can be written as $\Delta\lambda = \lambda - \lambda_0)/\lambda_0$. The detecting plane is chosen to be at the optimal phase imaging distance corresponding to the central wavelength λ_0, i.e. $\alpha = Z_{R0}/10 = 1/(20\lambda_0\mu^2)$=5cm. The normalized intensity distribution of image and the retrieved phase along the x axis are shown in Fig.3, with relative wavelength difference $\Delta\lambda$=0, $\pm$0.1%, $\pm$1%, $\pm$10%, $\pm$20% respectively. Evidently, the visibility of the image and the retrieved phase are almost the same as those in the use of the radiation of central wavelength when $\Delta\lambda$ is in a range of $\pm$1%. If the polychromatic radiation with every component of the wavelength having the same magnitude as that of the central wavelength is used, the maximum wavelength difference of $\pm 1\%\lambda_0$ has little effect on the image and the reconstructed phase. When $\Delta\lambda$ is beyond $\pm$20%, it will be impossible to obtain a discernible image, and the retrieved phase cannot map the original phase distribution at all. Gureyev *et al* used multi-energy method to retrieve the phase and the attenuation coefficient of the sample,[24] and they detected the image in the same observing plane even with a wavelength difference of $20\%\lambda_0$. If they had chosen the optimal phase imaging distance corresponding to different wavelengths as the detecting distance, the retrieved phase corresponding to a certain feature spatial frequency of a sample would have been more reliable.

Generally, for the polychromatic radiation, the radiation intensity at the central wavelength dominates over the whole intensity; the farther the wavelength away from the central one, the less its contribution to the radiation intensity is. Therefore, the maximum wavelength difference $\Delta\lambda$ in a polychromatic x-ray wave allowing for phase retrieval can be slightly lager than $\pm 1\%\lambda_0$. Figure 3 also shows that for the same magnitude of relative wavelength difference $|\Delta\lambda|$, the x-ray with a larger wavelength $\lambda = \lambda_0 + |\Delta\lambda|$ introduces more distortion to the phase contrast image and the retrieved phase. So better results can be obtained by choosing the optimal phase imaging distance corresponding to a larger wavelength as the detecting distance.

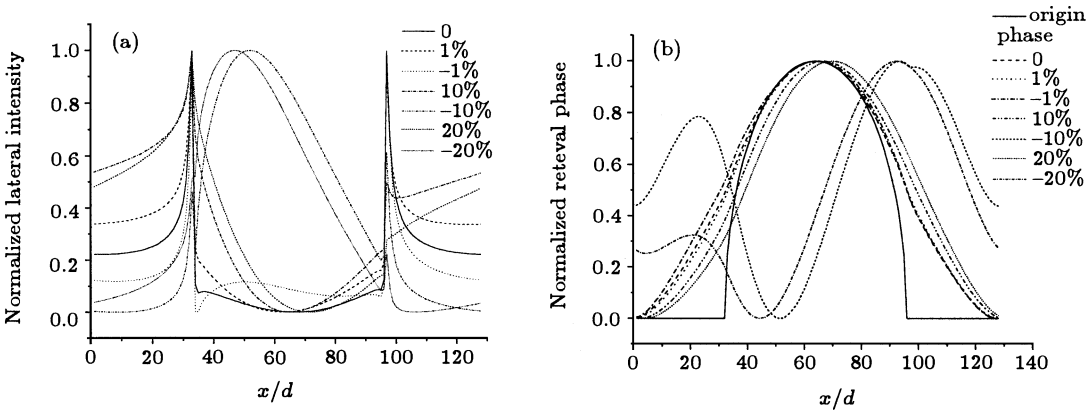


Fig.3. Intensity distribution of phase contrast image (a) and retrieved phase (b) along the x axis with the radiation wavelength λ satisfying $\Delta\lambda = (\lambda - \lambda_0)/\lambda_0 = 0, \pm 0.1\%, \pm 1\%, \pm 10\%, \pm 20\%$ respectively.

Finally, we give an ocular view of phase contrast image taken at the optimal phase imaging distance and the retrieved phase illuminated by a monochromatic plane wave. The sample then is a pure phase object with phase distribution in Fig.4(a). The intensity distribution in the image plane is shown in Fig.4(b) on a grid with 64×64 pixels with other experimental parameters being the same as those in Fig.2. For a comparison, we also plotted in Fig.4(c) the calculated distribution of the phase Laplacian $\nabla_\perp^2 \varphi(r_\perp, 0, \lambda_0)$, which is obviously almost identical with the intensity distribution in the image plane. The retrieved phase is shown in Fig.4(d). Again, it is in agreement with the original phase in Fig.4(a). The error between original phase and reconstructed phase is due primarily to the higher-order diffraction terms omitted in the derivation from Eq.(2) to Eq.(4).

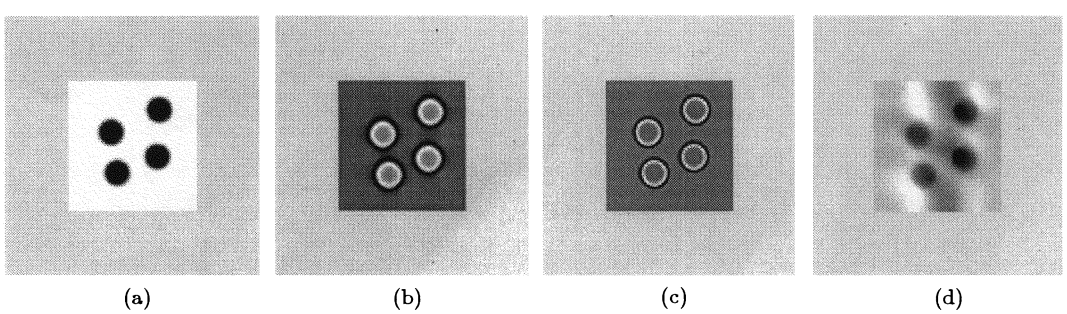


Fig.4. Phase contrast image (b) and retrieved phase distribution (d) of an object with phase distribution of (a); (c) shows the Laplacian of original phase distribution for a comparison with (b).

As far as phase retrieval methods are concerned, TEI is effective in the near field (Fresnel number $\gg 1$). But when it comes to the middle field (Fresnel number ≈ 1) and far field (Fresnel number $\ll 1$), TIE is no longer valid. The image measured in the middle field used for phase retrieval should be based on the combination of TIE and GSF algorithm (Gerchberg–Saxton Fienup algorithm),[16,17] or on SE algorithm[18,19] (simultaneous equation algorithm). In the far field, GSF algorithm is the best choice.

5. Conclusions

We have given another form of the equation for the intensity distribution of an image in the Fresnel region of a phase object illuminated by a monochromatic plane wave. The influences of detecting distance and polychromatic radiation on the phase contrast image are described by the derived formula. The phase distribution in the transmitted beam can be recovered by the solution of TIE. To our knowledge, it is the first time that the influences of polychromatic radiation on the TIE-based phase retrieval are considered and the maximum wavelength difference permitted is estimated. We have given a formula for optimal phase imaging distance as a function of wavelength of radiation and spatial resolution of the sample. Some illustrations of the optimal phase image for simulated data have also been presented. Different feature spa-

tial frequency of the object corresponds to different optimal phase imaging distance for a certain radiation wavelength. We can adjust the detecting plane according to the requirements for the sample to be measured. The introduction of optimal imaging distance gives convenience to the determination of detecting distance under the requirements for feature spatial resolution, which increases the efficiency and decreases the blindness in experiments. Though the optimal imaging distance is investigated just in a trial-and-error way, the obtained result is useful. The rigorous analytical derivation should be one subject for our future research.

References

[1] Bonse U and Hart M 1965 *Appl. Phys. Lett.* **6** 155

[2] Ando M and Hosoya S 1972 in Proceedings of the International Conference of X ray Optics and Microanalysis, Tokyo, p63

[3] Momose A 1995 *Nucl. Instrum. Methods Phys. Res.* A **353** 622

[4] Forster E, Goetz K and Zaunseil P 1980 *Krist. Tech.* **15** 973

[5] Davis T J, Gao D, Gureyev T E, Stevenson A W and Wilkins S W 1995 *Nature* **373** 595

[6] Gao D, Davis T J and Wilkins S W 1995 *Aust. J. Phys.* **48** 103

[7] Ingal V N and Beliaecskaya E A 1995 *J. Phys.* D **28** 2314

[8] Snigirev A, Snigireva I, Kohn V, Kuznetsov S and Schelokov I 1995 *Rev. Sci. Instrum.* **66** 5486

[9] Cloetens P, Barrett R, Baruchel J, Guigay J P and Schlenker M 1996 *J. Phys.* D **29** 133

[10] Chen M *et al* 2004 *Acta Phys. Sin.* **53** 2953 (in Chinese)

[11] Cheng J *et al* 1999 *Acta Opt. Sin.* **19** 596 (in Chinese)

[12] Yu H *et al* 2003 *Acta Opt. Sin.* **23** 390 (in Chinese)

[13] Wilkins S W, Gureyv T E, Gao D, Pogany A and Stevenson A W 1996 *Nature* (Landon) **384** 335

[14] Pogany A, Gao D and Wilkins S W 1997 *Rev. Sci. Instrum.* **68** 2774

[15] Raven C, Snigirev A, Spanne P, Souvorov A and Kohn V 1996 *Appl. Phy. Lett.* **69** 1826

[16] Fienup J R 1982 *Appl. Opt.* **21** 2758

[17] Gureyev T E 2003 *Opt. Communications* **220** 49

[18] Nakajima N 2004 *Appl. Opt.* **43** 1710

[19] Nakajima N 2003 *Appl. Opt.* **42** 2492

[20] Bronnikov A V 2002 *J. Opt. Soc. Am.* A **19** 472

[21] Teague M R 1983 *J. Opt. Soc. Am.* A **73** 1434

[22] Arndt U W and Willis B T M 1966 *Single Crystal Diffractometry* (Cambridge: Cambridge University Press) p185

[23] Gureyev T E and Nugent K A 1996 *J. Opt. Soc. Am.* A **13** 1670

[24] Gureyev T E, Mayo S, Wilkin S W, Paganin D and Stevenson A W 2001 *Phys. Rev. Lett.* **86** 5827